Shortest paths on systems with power-law distributed long-range connections

C. F. Moukarzel[1,2,*] and M. Argollo de Menezes[2]

[1]*Departamento de Física Aplicada, CINVESTAV del IPN, Avenue Tecnológico Km. 6, 97310 Mérida, Yucatán, Mexico*
[2]*Instituto de Física, Universidade Federal Fluminense, Avenue Litorânea s/n, 24210-340 Niterói, RJ, Brazil*

We discuss shortest-path lengths $\ell(r)$ on periodic rings of size L supplemented with an average of pL randomly located long-range links whose lengths are distributed according to $P_l \sim l^{-\mu}$. Using rescaling arguments and numerical simulation on systems of up to 10^7 sites, we show that a characteristic length ξ exists such that $\ell(r) \sim r$ for $r < \xi$ but $\ell(r) \sim r^{\theta_s(\mu)}$ for $r \gg \xi$. For small p we find that the shortest-path length satisfies the scaling relation $\ell(r,\mu,p)/\xi = f(\mu, r/\xi)$. Three regions with different asymptotic behaviors are found, respectively: (a) $\mu > 2$ where $\theta_s = 1$, (b) $1 < \mu < 2$ where $0 < \theta_s(\mu) < 1/2$, and (c) $\mu < 1$ where $\ell(r)$ behaves logarithmically, i.e., $\theta_s = 0$. The characteristic length ξ is of the form $\xi \sim p^{-\nu}$ with $\nu = 1/(2-\mu)$ in region (b), but depends on L as well in region (c). A directed model of shortest paths is solved and compared with numerical results.

I. INTRODUCTION

It has been known for long that slowly decaying long-ranged (LR) interactions can drastically change the critical behavior of a system. A well studied example is the one-dimensional (1D) Ising model with $J(r) \sim r^{-\mu}$ [1–10], which is relevant for the Kondo problem [11,12] among others. If $\mu > 2$ there is no ordered phase at any finite temperature, the same as if only short-ranged interactions were present. When $\mu = 2$ the magnetization undergoes a finite jump at $T_c > 0$, while all derivatives of the free energy remain finite (essential singularity). When $\mu < 2$ the model displays a second-order phase transition with μ-dependent critical indices, which take their classical, or mean-field (MF) values for $\mu < 1.5$. On approach to $\mu = 2$ from below, the correlation-length exponent diverges, signaling the appearance of an essential singularity. This divergence is of the form $\nu \sim (2-\mu)^{-1/2}$ [4] for Ising and $(2-\mu)^{-1}$ for n-component models with $n > 1$ [but see Ref. [13], where $\nu \sim (2-\mu)^{-1} \, \forall n$ is suggested]. A comprehensive account of what is known for Ising systems with LR interactions has been given by Luijten and Blote [8].

For d-dimensional n-component systems with ferromagnetic interactions decaying as $1/r^{d+\sigma}$, Fisher, Ma, and Nickel [3] propose that the lower critical decay rate is given by $\sigma = d/2$, or equivalently that the upper critical dimension is $d_u = 2\sigma$. For $\sigma < d/2$ the critical indices take their MF values, for $d/2 < \sigma < 2$ they are σ dependent, and for $\sigma > 2$ they take their short-range (SR) values. Similar investigations have been conducted for Potts [13–16], Heisenberg [17–22], and other [23,24] models.

The following picture is often found: for small enough decay rate μ, MF indices are obtained. Upon increasing μ a regime follows where critical indices change continuously with μ until finally SR indices are recovered. In a loose

sense one can say that the addition of LR interactions changes the "effective dimension" of the system, although in a way that may depend on the specific model considered. This idea has been exploited to study the scaling behavior of critical systems above their effective upper critical dimension d_u, while still working on lattices of low Euclidean dimension [7]. The connection between LR interactions and dimensionality was also briefly touched upon by Scalettar [25]. A possible way to define an effective dimension, which is in general model dependent, is to do so through the hyperscaling relation $(2-\alpha) = d\nu$, as [10,16] $d_{eff} = \nu^{-1}(2-\alpha)$.

An alternative paradigm for the problem of LR interactions considers systems on a d-dimensional lattice supplemented with randomly distributed LR bonds of unit strength, which are present with probability $p_{ij} \sim r_{ij}^{-\mu}$. Notice that in this case the system has disorder: it is the probability for a given bond to be present, and not its strength, that decays with distance. These two ways to introduce LR interactions, decaying strength (DS) and decaying probability (DP), are not, in principle, equivalent: it is well known that disorder may change the critical behavior if the specific-heat exponent α is positive. In this case, the critical indices of a statistical model on DS and DP networks with the same value of μ may differ.

The DP paradigm is on the other hand relevant for a number of problems in which connectivity, and not the strength of the interaction, is determinant of the physical behavior. Examples of problems of this kind are the magnetic [26] and conductive [27,28] properties of polymeric chains, where the probability of crosslinks between two monomers decays as a power law of the chemical distance between them, conduction in insulating matrices with one-dimensional conducting inclusions [29] whose length distribution is "broad," neural networks [30,31], geodesic propagation on spaces with topological singularities (wormholes), the spread of fire or diseases [32,33], etc.

Networks built according to the DP paradigm of LR interactions may be characterized entirely in geometrical (or topological) terms, because all bonds have the same strength. Thus it appears, for example, possible to define the relation-

*Corresponding author.
Email address: cristian@mda.cinvestav.mx

ship between effective dimension d_{eff} and decay rate μ of interactions in purely geometric terms for these networks.

A useful topological characterization of random networks is the *graph dimension* d_g, defined as follows: if $V(\ell)$ is the average number of sites that can be reached from a given one in ℓ steps between connected neighbors, then $V(\ell) \sim \ell^{d_g}$ asymptotically. We now let $\ell(r)$ be the average smallest number of links needed to join two points separated by an Euclidean distance r (the "shortest-path length"), which behaves asymptotically as r^{θ_s}, where θ_s is the shortest-path dimension [34]. Since $V(r) \sim r^d$, the above relations imply that $d_g = d/\theta_s$, and we see that the asymptotic behavior of $\ell(r)$ defines the graph dimension d_g.

In this work we study shortest-paths on DP networks, i.e., d-dimensional lattices with the addition of an average of p LR bonds (or *shortcuts*) per site, whose length is distributed according to $P_l \sim l^{-\mu}$. We shall concentrate mostly on the case $d = 1$, where numerical simulations are easiest. DP networks with power-law distributed LR bonds have been recently considered in one dimension both from the point of view of random walk properties [35] and shortest-path lengths [36], but for small system sizes. We will later discuss some of the conclusions in [36], which appear to need revision in the light of our results.

In Sec. II several definitions that are relevant for our problem of shortest-paths on 1D DP networks are given. Simple rescaling arguments are used in Sec. II A to show that $\mu = 2d$ is a critical decay rate, such that for $\mu > 2d$, LR bonds are unimportant on large scales. For $\mu < 2d$, on the other hand, when p is small these arguments predict the existence of a characteristic length $\xi \sim p^{-1/(2-\mu)}$, beyond which LR bonds are important. In Sec. II B a directed model is introduced for shortest-paths in 1D, which turns out to be exact for $\mu > 2$ and still provides a useful upper bound when $\mu < 2$. In Sec. III our extensive numerical results for shortest-path lengths $\ell(r)$ in one dimension are described and compared to theoretical predictions. Finally, Sec. IV contains a discussion of our results.

II. DP NETWORKS AND RESCALING

We start with an arbitrary d-dimensional lattice made up of $N = L^d$ sites, and its corresponding SR bonds. In addition to these, DP networks are defined to have an average of pL^d LR bonds, or *shortcuts*, whose lengths and locations are random. This is done in practice by letting one LR bond stem from each site i with probability p. The neighbor j at the other end of each LR bond is randomly chosen with a probability $P(j|i)$, that is a decaying function of the Euclidean distance $r_{ij} = |\vec{x}_i - \vec{x}_j|$ between sites i and j.

For a given realization of shortcuts, the shortest-path length ℓ_{ij} is defined as the minimum number of connected-neighbor steps needed to join sites i and j. This quantity is measured as a function of Euclidean distance r_{ij}, and averaged over disorder (realizations of shortcuts). After disorder average, $\ell(r)$ is the average "cost" of joining two points separated by an Euclidean distance r, and is defined as

$$\ell(r) = \sum_{ij} \langle \ell_{ij} \rangle \delta(r_{ij} - r) / \sum_{ij} \delta(r_{ij} - r), \qquad (1)$$

where $\langle \rangle$ means disorder average.

A. Rescaling

Consider now dividing the d-dimensional lattice into "blocks" of linear dimension b, such that $1 \ll b \ll L$ and regard two sites I and J of this new lattice to be connected by a shortcut if *any* pair $\{i \in I, j \in J\}$ is connected by a shortcut. We allow for at most one shortcut between rescaled sites since, for the purpose of shortest paths, the only fact that matters is whether two sites are connected or not. If the original pairs ij are connected by a shortcut with probability p_{ij}, the rescaled probability $\tilde{q}_{IJ} = 1 - \tilde{p}_{IJ}$ for blocks I and J not to be connected is given by

$$\tilde{q}_{IJ} = \prod_{i \in I, \, j \in J} (1 - p_{ij}) = \prod_{i \in I, \, j \in J} q_{ij}, \qquad (2)$$

which for large distances $|i - j| \gg b$ can be approximated as $\tilde{q}_{IJ} = q_{ij}^{b^{2d}}$. This can be written as $\tilde{q}(r/b) = [q(r)]^{b^{2d}}$ and, therefore, $\lambda(r) = \ln q(r)$ transforms in a simple way under rescaling,

$$\tilde{\lambda}(r/b) = b^{2d} \lambda(r). \qquad (3)$$

Thus

$$p(r) = (1 - e^{-\rho/r^\mu}), \qquad (4)$$

retains its functional form under rescaling, i.e.,

$$\tilde{p}(r) = (1 - e^{-\tilde{\rho}/r^\mu}), \qquad (5)$$

with $\tilde{\rho} = b^{(2d-\mu)} \rho$. The condition that the system contains a total of pL^d LR bonds is ensured by imposing

$$p = S_d \int_1^L p(r) r^{d-1} dr, \qquad (6)$$

where S_d is the surface of a d-dimensional hypersphere of radius one. This relationship fixes ρ as a function of p and L. In the limit of small p, ρ turns out to be proportional to p. Notice that, because of the multiplicative rescaling Eq. (2), a pure power law is not strictly invariant under rescaling. But the true invariant distribution Eq. (4) can be very well approximated by a power law for large distances r such that $\rho/r^\mu \ll 1$. Restricting ourselves to the limit of small ρ (or p) we can thus work with a power-law distribution of shortcut lengths. In the following we consider

$$p(r) = C \frac{p}{r^\mu}, \qquad (7)$$

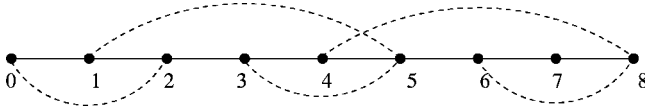where the normalization constant C is chosen so as to satisfy Eq. (6). In the Appendix we show that p rescales as

FIG. 1. Full lines are SR bonds, dashed lines are LR bonds. One possible shortest path between 0 and 8 is {0-1,1-5,5-4,4-8} and has length 4. The naive path uses all rightwards LR bonds available at each site, i.e., {0-2,2-3,3-5,5-6,6-8} and has length 5 in this example.

$$\tilde{p} = b^{y_p} p, \tag{8}$$

with

$$y_p = \begin{cases} d & \text{for} \quad \mu \leq d, \\ 2d - \mu & \text{for} \quad \mu > d. \end{cases} \tag{9}$$

Notice that expressions similar to Eqs. (8) and (9) give the renormalized coupling constant of the one-dimensional LR Ising model at low temperatures [6].

It follows that $p=0$ is a line of fixed points in the μ, p space of parameters. For $\mu < 2d$ this fixed line is repulsive, and becomes attractive for $\mu > 2d$. Thus for $\mu > 2d$ the density of LR bonds is renormalized to zero under rescaling, and $\mu_c = 2d$ is the upper critical decay rate above which LR bonds are irrelevant, and SR behavior is recovered.

B. Naive paths: An approximate model in one dimension

Consider a directed path that starts at $t=0$ from $x_0=0$, proceeds always to the right, and is built by using at each site any LR bond available, provided this bond does not take the path further to the right than r. We call the path so defined the "naive path" between 0 and r. As compared with the actual shortest path, this construction neglects the possibility of turnbacks, or that certain LR bonds may not be used (see Fig. 1). We will later see that under certain circumstances, the naive-path approximation gives a reasonable estimate for shortest-path lengths. But even if this is not the case, the former constitutes an upper bound for the shortest-path length, and thus still provides useful information. The naive-path length $\ell_n(r)$ is the number of time steps it takes to reach r, and can be estimated in the following way. At time t the walker sits at site x_t. From this site, with probability p a LR bond (of random length l_t) stems rightwards. The walker now proceeds along this LR bond, provided it does not go further to the right than r. The joint probability $\tilde{p}_t$ that a bond is present at x_t, and its length is not larger than $r-x_t$ is

$$\tilde{p}_t = p \sum_{l=1}^{r-x_t} P_l. \tag{10}$$

Thus at time t the walker goes one unit to the right with probability $\tilde{q}_t = 1 - \tilde{p}_t$, and l_t units with probability $\tilde{p}_t$. Therefore, in average

$$x_t = x_{t-1} + 1 + \tilde{p}_t(\bar{l}_t - 1), \tag{11}$$

where $\bar{l}_t$ is the average length of a LR bond, which is not larger than $r - x_t$, i.e.,

$$\bar{l}_t = \frac{\sum_{l=1}^{r-x_t} l P_l}{\sum_{l=1}^{r-x_t} P_l} = \frac{p}{\tilde{p}} \sum_{l=1}^{r-x_t} l P_l. \tag{12}$$

Thus Eq. (11) reads

$$x_t = x_{t-1} + 1 + p G(r - x_t), \tag{13}$$

where

$$G(n) = \sum_{l=1}^{n} (l-1) P_l. \tag{14}$$

Within a continuous-time, continuous-space approximation we put

$$\dot{x}(t) = 1 + p G(r - x(t)), \tag{15}$$

which shall be solved with boundary conditions $x(t=0) = 0$ and $x(t=\ell_n(r)-1) = r-1$ [notice that Eqs. (10) and (12) are only defined for $x_t \leq r-1$]. This can be formally integrated to give

$$\ell_n(r) = 1 + \int_1^r \frac{dx}{1 + p G(x)}. \tag{16}$$

We will analyze this result and compare it with our numerical results in the following sections.

III. NUMERICAL RESULTS IN ONE DIMENSION

In this section, numerical results are presented for periodic rings of up to 10^7 sites. One LR bond stems from each site with probability $p \leq 1$. Its random length l is obtained by first generating a real random variable z such that $1 \leq z < (L/2+1)$ with $P(z) \sim z^{-\mu}$, and then taking its integer part: $l = \text{Int}(z)$. Lattice sizes are $L_k = 10^{3+k/2}$ for $k = 0,1,\ldots,8$. The density of LR bonds is $p = 0.001, 0.003, 0.01, 0.033, 0.1$, and 1.0. Shortest paths are identified by breadth-first-search [37,38], and averages are taken over 10^4 samples. Altogether the results presented in this work involve an amount of computational work approximately equivalent to finding of the shortest paths on a single system containing 10^{12} sites. Figures 2, 3, and 4 show average shortest-path lengths $\ell(r)$, respectively, for the regions: $0 \leq \mu \leq 1$, $1 < \mu < 2$, and $\mu \geq 2$.

It is apparent in these plots that $\ell(r)$ does not depend on system size L (only on p and μ) for $\mu > 1$. This is consistent with the fact that the probability $P(r)$ for two sites separated by an Euclidean distance r to be connected by a LR bond does not depend on L when $\mu > d$. [See Eq. (A6)]. In comparison, when $\mu < d$ one has that $P(r)$ decays to zero with system size as $L^{-(d-\mu)}$. This scale dependence in the connectivity properties is evidenced by the size dependence of $\ell(r)$ when $\mu < 1$ in Fig. 2.

A second noticeable feature is that for all $\mu < 2$ a characteristic size ξ exists with the following property: For $r \ll \xi$,
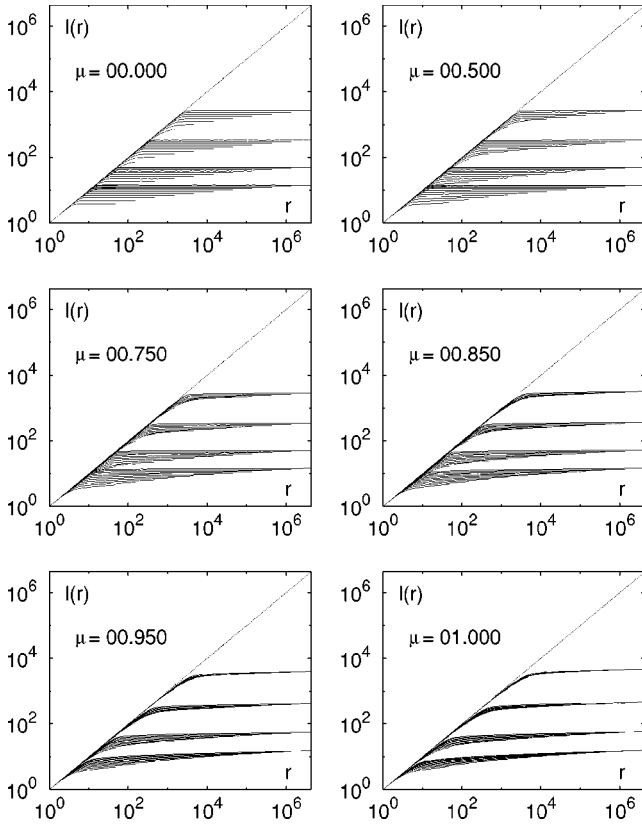
FIG. 2. Average shortest-path length $\ell(r)$ vs r. Numerical averages (full lines) over 10^4 samples are shown for systems of size $L_k = 10^{3+k/2}$ with $k = 0, 1, \ldots, 8$. The dashed line is $\ell(r) = r$. The local density p of LR bonds is $p = 10^{-3}$, 10^{-2}, 10^{-1}, and 1. The different cases can be told apart by noticing that larger values of p result in lower values of ℓ.

$\ell(r) \approx r$, while for $r > \xi$, $\ell(r)$ grows asymptotically slower than r; in general as r^{θ_s} with $\theta_s < 1$. This characteristic size ξ is a function of p and μ for $1 < \mu < 2$, but also depends on L for $\mu < 1$.

A. The $\mu > 2$ regime

As seen in Sec. II, for $\mu > 2$ the density of LR bonds rescales to zero, i.e., $p = 0$ is an attractive fixed line. Thus one does not expect LR bonds to modify the effective geometry of the lattice in this regime. In fact it is found (Fig. 4) that $\ell(r) \propto r$ at large distances, and thus $d_{eff} = d$ in this regime, although the coefficient of proportionality depends on μ and p, in general. Our directed model (naive paths) described in Sec. II B gives exact results in this regime as we now show.

Naive paths when $\mu > 2$

When $\mu > 2$, $G(x)$ in Eq. (16) grows monotonically from $G(1) = 0$ to $G(\infty) = \bar{l} - 1$. Thus asymptotically $\ell_n(r) = r/[1 + p(\bar{l} - 1)]$. In order to obtain the short-distance behavior we may approximate, to first order in $p(\bar{l} - 1)$,

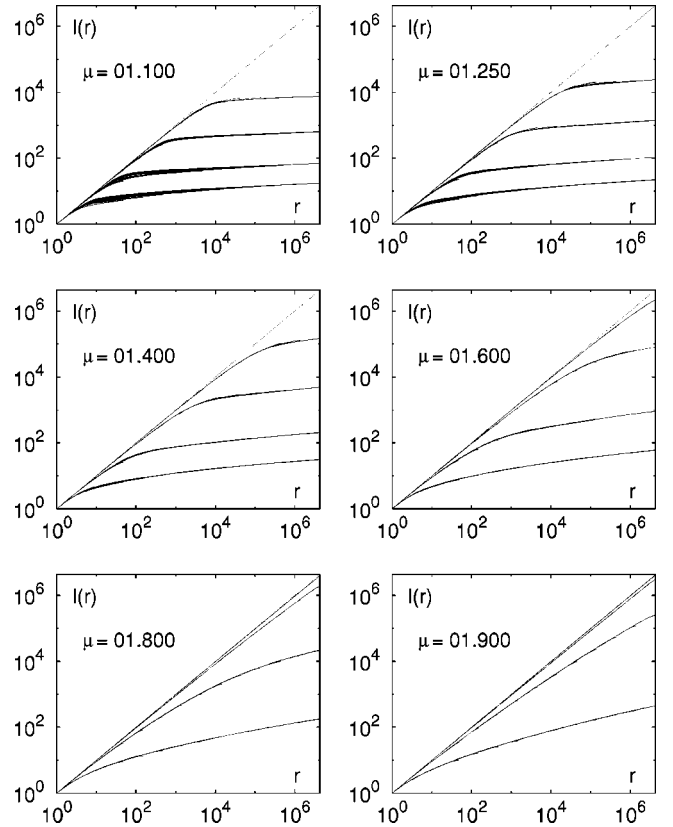$$[1 + pG(x)]^{-1} \approx 1 - pG(x). \tag{17}$$

FIG. 3. Same as Fig. 2, for $1 < \mu < 2$.

Equation (16) now reads

$$\ell_n(r) \approx r[1 - p\Phi(r)], \tag{18}$$

where

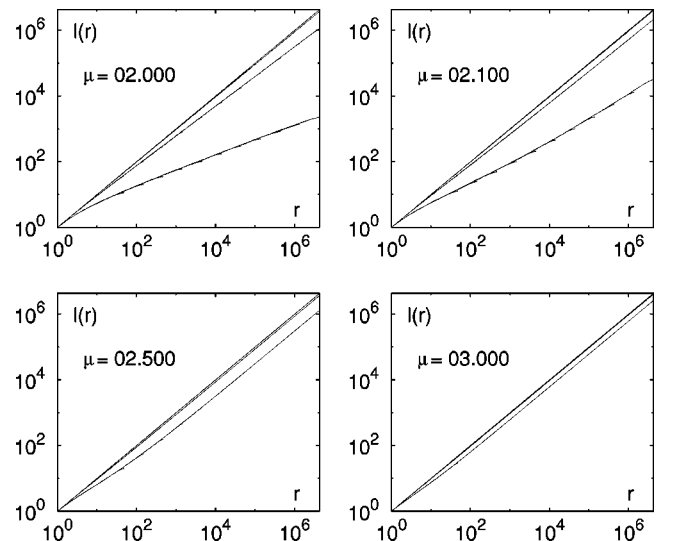$$\Phi(r) = \frac{1}{r} \int_1^r G(x)\,dx \tag{19}$$

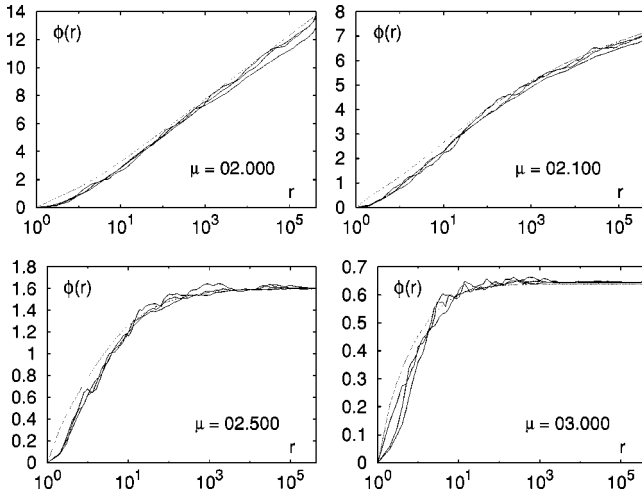FIG. 4. Same as Fig. 2, for $\mu \geq 2$.

FIG. 5. For $\mu > 2$ shortest path lengths $\ell(r)$ are well approximated by Eq. (18) with Φ given by Eq. (19). Shown in this plot are our numerical results (solid lines) for $\Phi(r) = p^{-1}[1 - \ell(r)/r]$ for small densities of LR bonds: $p = 10^{-3}$, 3×10^{-2}, and 10^{-2}. The dashed line indicates our analytic result, Eq. (A10).

is a p-independent function that converges to $\bar{l} - 1$ for large r. Equation (19) can be integrated (see Appendix A 3), and the comparison between analytical and numerical results is done in Fig. 5. The coincidence betweeen the naive-path model and numerical results is very good even at $\mu = 2$. Thus we conclude that in the $\mu \geq 2$ regime and when p is small, shortest paths are essentially naive paths.

B. The $1 < \mu < 2$ regime

In Sec. II A we saw that $p = 0$ is a repulsive fixed point for all $\mu < 2$ in one dimension. Because of the rescaling law Eq. (8), one expects a lengthscale $\xi \sim p^{-1/y_p} = p^{-1/(2-\mu)}$ to be relevant for the behavior of $\ell(r)$ as $p \to 0$. For $r \ll \xi$, the $p = 0$ fixed point is dominant [for which $\ell(r) = r$] while for $r \gg \xi$ the effects of LR bonds may become visible [$\ell(r)$ shorter than r].

1. Naive paths when $1 < \mu < 2$

For $\mu < 2$, $\bar{l}$ is not well defined. However the average length $\bar{l}_t$ of a LR bond not larger than $r - x_t$ is well defined and given by Eq. (12). Notice that $G(r)$ now grows as $r^{2-\mu}$. Equation (16) is still valid for naive paths, and one gets in the limit of large r that $\ell(r) \sim r^{\mu-1}$, i.e., $\theta_s^{naive} = \mu - 1$. It turns out that actual shortest paths are shorter than naive paths for $\mu < 2$, i.e, $\theta_s^{naive} = \mu - 1$ is only an upper bound for θ_s (see Sec. III B 3).

Although the naive-path model fails to predict the asymptotic behavior of $\ell(r)$, it can nevertheless still help us determine the characteristic length ξ beyond which $\ell(r)/r \to 0$. Keeping just the fastest-growing term in $G(y)$ [Eq. (18)] and equating $pG(\xi) \approx 1$, one gets $\xi \sim p^{-1/(2-\mu)}$, in full accordance with rescaling arguments in Sec. II A and at the beginning of this section. We show next that this is verified numerically.
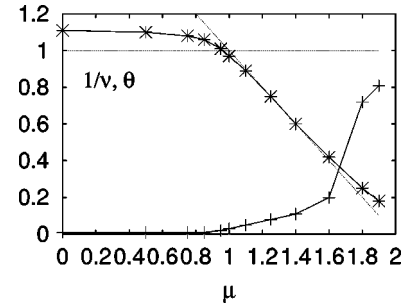

FIG. 6. Numerical estimates for $1/\nu$ (asterisks) and θ (pluses), obtained by fitting Eq. (22) to our data for $L = 10^7$ and $p = 0.001$, 0.003, and 0.010. The dotted lines are $1/\nu = 2 - \mu$ and $1/\nu = 1$.

2. A single characteristic length ξ

In this section we test the hypothesis that a single length-scale $\xi(p)$ dictates the behavior of $\ell(r)$ in the limit of small p, and show that for $1 \leq \mu \leq 2$ this lengthscale is $\xi = p^{-1/(2-\mu)}$, in accordance with rescaling arguments [Eq. (8)] and naive-path predictions. We propose that, for $p \to 0$,

$$\ell(r,\mu,p)/\xi = f(\mu, r/\xi), \tag{20}$$

where $\xi \sim p^{-\nu}$, and

$$f(\mu, x) \propto \begin{cases} x & \text{for} \quad x \ll 1, \\ x^{\theta_s(\mu)} & \text{for} \quad x \gg 1. \end{cases} \tag{21}$$

This means that all p-dependence of $\ell(r)$ is contained in $\xi(p)$.

By comparison with our numerical results we find that $f(x)$ can be well approximated by $f(x) = x/[1 + Cx^{(1-\theta_s)}]$. Therefore,

$$\ell(r)/\xi \approx \frac{r/\xi}{1 + C(r/\xi)^{1-\theta_s}}, \tag{22}$$

or, equivalently,

$$\frac{r}{\ell(r)} - 1 \approx C[rp^\nu]^{1-\theta_s}, \tag{23}$$

provide a good approximation to our numerical results. We fit Eq. (23) to our numerical data for $L = 10^7$ and $p = 0.001, 0.003, 0.010$ simultaneously [using $\nu(\mu)$, $\theta_s(\mu)$, and $C(\mu)$ as fitting parameters], and find ν and θ_s as shown in Fig. 6. These results are entirely consistent with $1/\nu = (2 - \mu)$ for $1 < \mu < 2$. Larger values of p are found not to follow Eq. (20) satisfactorily, therefore, we must regard this scaling expression as only valid in the $p \to 0$ limit.

A plot of $\ell(r)/\xi(p)$ vs r/ξ is shown in Fig. 7 for $p = 0.001$, 0.003, and 0.010. The fact that all three values of p collapse neatly onto one single curve suffices to verify the correctness of our scaling ansatz Eq. (20) for small p. The specific form of $f(x)$ chosen in Eq. (22) should however only be regarded as empiric.

Although for $\mu < 1$ we do not expect Eq. (23) to hold (since then ξ has an additional L-dependence not included in
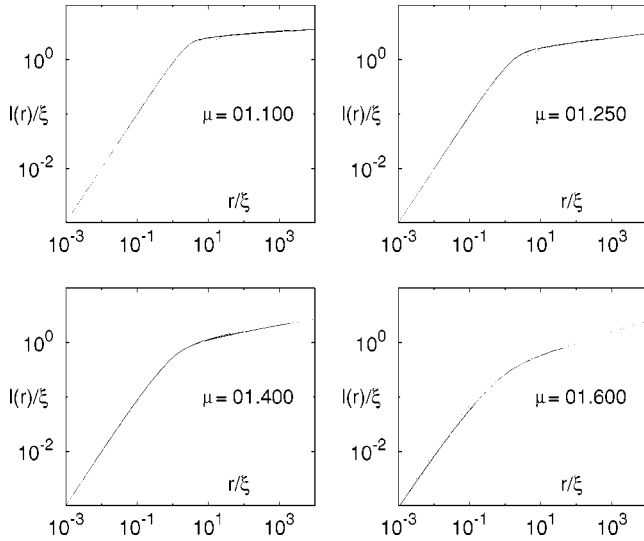
FIG. 7. Data collapse of $\ell(r)$, showing plots of ℓ/ξ vs r/ξ with $\xi(p)=p^{-1/(2-\mu)}$, for $p=0.001$, 0.003, and 0.010. The dashed line is our approximate expression Eq. (22). For larger values of $\mu<2$ and the same values of p, the characteristic size is much larger than 10^7.

FIG. 8. Asymptotic exponent θ_s vs decay exponent μ, obtained from power-law fit of the large-r behavior of $\ell(r)$, for L of the form $L_k=10^{3+k/2}$, $k=0,1,\ldots,8$, and for the values of densities of LR bonds p indicated in the respective plots. Lines are guides to the eye. In all four cases, the steepest curves correspond to larger values of L.

these expressions, see Sec. III C), a fit of the data gives $\nu \approx 1$, indicating that the p dependence of the characteristic size ξ is of the form p^{-1} in this region. This is again consistent with Eq. (9). We will discuss the regime $\mu<1$ in detail later in Sec. III C. When p is small and μ is close to 2, ξ grows too large. Consequently neither ξ nor θ can be correctly estimated for $\mu>1.6$. Consider for example $p=10^{-2}$. One then has $\xi\sim10^5$ for $\mu=1.6$, but $\xi\sim10^{10}$, well beyond our present reach, for $\mu=1.8$. Thus the estimates for θ and $1/\nu$ in Fig. 6 are to be disregarded for $\mu>1.6$.

3. Asymptotic exponent θ_s

When $r\gg\xi$, we find that $\ell(r)$ grows asymptotically as r^{θ_s}. The shortest-path dimension θ_s depends on μ only, goes to zero as $\mu\to1^+$ and jumps discontinuously to $\theta_s=1$ at $\mu=2^-$. We estimate θ_s by two different methods. A simple power-law fit of the large-r behavior of $\ell(r,\mu,p)$ gives the estimates shown in Fig. 8 for L ranging from 10^3 to 10^7 and several values of p. Strong finite-size corrections affect the smaller values of p, for which $\xi\gg L$ when $\mu\to2$. However, for large L all these estimates are seen to converge to similar values within numerical accuracy.

The second method chosen to estimate θ_s consists in fitting our numerical data using Eq. (23) but with $\nu=1/(2-\mu)$ instead of taking ν as a fitting parameter as in Fig. 6. Fits of our data for $L=10^7$ and $p=0.001,0.003,0.010$ produce the values of θ_s shown in Fig. 9. Again the results obtained for $\mu>1.6$ are to be disregarded since ξ is much larger than L for these values of p. A naive interpretation of the results in Fig. 8, for any fixed value of L, could lead one to believe that the transition between linear behavior [$\ell(r)\propto r$] and sublinear behavior [$\ell(r)/r\to0$ for $r\to\infty$] happens at a p-dependent boundary $\mu_c(p)$ [36]. However, a more careful numerical analysis shows that this transition happens
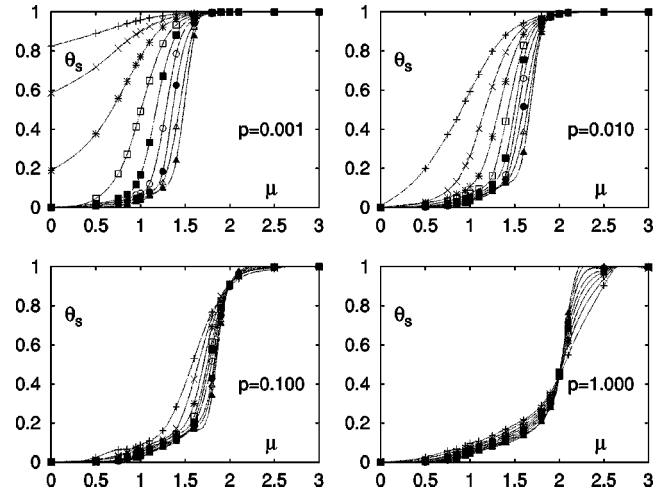
at $\mu_c=2$ for all p in the thermodynamic limit, as predicted by rescaling arguments (Sec. II A) and the naive-path model (Sec. II B). This appears to be in partial disagreement with recent work of Sen and Chakrabarti (SC) [36], where the "regular lattice behavior" [$\ell(L)\sim L$] is claimed to extend below $\mu=2$ for small values of p. SC explain what they call the lack of small-world behavior in lattice polymers as being a consequence of the small number of LR connections (small p). Based on the analysis of $\ell(L)$ on relatively small ($L=10^4$) systems, SC conclude that there is a p-dependent phase boundary $\mu_c(p)<2$, and show that several lattice polymer models lay marginally on the regular lattice [$\ell(L)\propto L$] side of this boundary. Our extensive numerical results and analytic considerations however show that $\mu=2$ is the critical decay rate below which $\ell(r)\ll r$, for *any* density p of LR bonds. The p-dependent boundary that SC observe is just a logarithmically slow finite-size effect. At sufficiently low
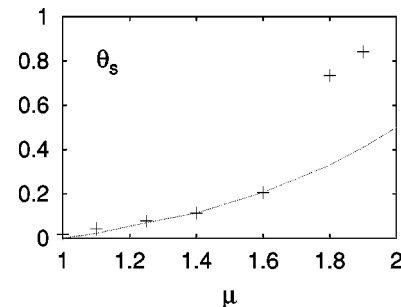

FIG. 9. Numerical estimates for the asymptotic exponent θ_s (pluses) in Eq. (22), resulting from fits of our data for $L=10^7$ and $p=0.001$, 0.003, and 0.010 with $\xi=p^{-1/(2-\mu)}$. The rightmost two points, for μ larger than 1.6, suffer from strong finite-size effects and should be disregarded. The dotted line sketches what we believe is the true value of $\theta_s(\mu)$. The discontinuity at $\mu=2$ is suggested by the behavior of the $p=1.0$ results in Fig. 8.

values of p, and for μ close to but lower than two, the characteristic length $\xi(\mu,p)$ is larger than L and thus $\ell(L) \propto L$. Equating $\xi = p^{-1/(2-\mu)} = L$, one obtains an apparent boundary $\mu^*(p) = 2 - \ln(1/p)/\ln(L)$ that converges logarithmically slowly to $\mu_c = 2$. Replacing $L = 10^4$, this last expression follows closely the boundary reported by SC in Fig. 3 of Ref. [36].

There is a second aspect of Ref. [36] with which our findings seem to be in disagreement. According to SC, there are only two phases regarding the asymptotic behavior of $\ell(r)$. A logarithmic phase, $\ell(L) \propto \ln(L)$, for $\mu < \mu^*(p) \approx 2$, and a linear phase for $\mu > \mu^*(p)$. Our numerical evidence however suggests a more complex scenario. For $1 < \mu < 2$ we find that $\ell(r) \propto r^{\theta_s}$ with θ_s small but nonzero (Fig. 9), and only for $\mu < 1$ ℓ becomes logarithmic (see Sec. III C).

C. The $0 \le \mu < 1$ regime

The data in Fig. 2 clearly show that $\ell(r)$ depends on system size L if $0 \le \mu < 1$. In the specific case $\mu = 0$, each of the $L^{2d}/2$ possible LR bonds is present with the same probability pL^{-d}. This corresponds to a d-dimensional lattice supplemented with pL^d LR bonds whose ends are randomly chosen, and goes under the name of small-world (SW) network [32,39–47]. In particular it was recently found [32,44] that on SW networks ($\mu = 0$) there is still a single characteristic length r_c dictating the behavior of $\ell(r)$, but it depends both on L and p, and diverges as $L \to \infty$, in any dimension d. Analytic calculations [32] confirmed by numerical measurement [44,47] show that, in d dimensions,

$$\ell(r) = \begin{cases} r & \text{for} \quad r < r_c, \\ r_c & \text{for} \quad r > r_c, \end{cases} \tag{24}$$

where $r_c \sim p^{-1/d} \ln(KpL^d)$ with K a constant.

In the particular case $d = 1$ one has $r_c(\mu=0,L,p) \sim p^{-1} \ln(4pL)$. So the $\mu = 0$ case is relatively simple, with $\ell(r) = r$ for $r < \ln(4pL)/p$ and $\ell(r) = \ln(4pL)/p$ for large r.

By inspection of Fig. 2 one concludes that r_c depends on L as well as on p, μ in the whole $0 \le \mu < 1$ range. When $\mu = 1$ however, the characteristic length dictating the behavior of $\ell(r)$ is $\xi = p^{-1}$, and no longer L dependent, as shown in Sec. III B. Guided by these observations, we now propose an empirical expression for r_c in terms of L, p, μ in the whole $0 \le \mu \le 1$ range. This expression has to result in $\xi = p^{-1}$ when $\mu \to 1$, and $r_c \sim p^{-1} \ln(pL)$ when $\mu \to 0$. It is easy to verify that

$$r_c(\mu,p,L) = p^{-1} \ln[4(pL)^{(1-\mu)}]/\ln(4) \tag{25}$$

satisfies both requirements. We find that this empirical expression gives acceptable results for small p. In Fig. 10 we show $\ell(r)/r_c$ r/r_c with r_c given by Eq. (25), for all values of L ranging from 10^3 to 10^7 and $p = 0.001$, 0.003, and 0.010. The acceptable collapse of all data supports the validity of Eq. (25) reasonably well.

We find that $\ell(L)$ grows asymptotically as $\ln(L)$ for $0 < \mu \le 1$. The naive-path model already predicts a logarithmic behavior at $\mu = 1$ as the following shows. For $\mu = 1$ one has
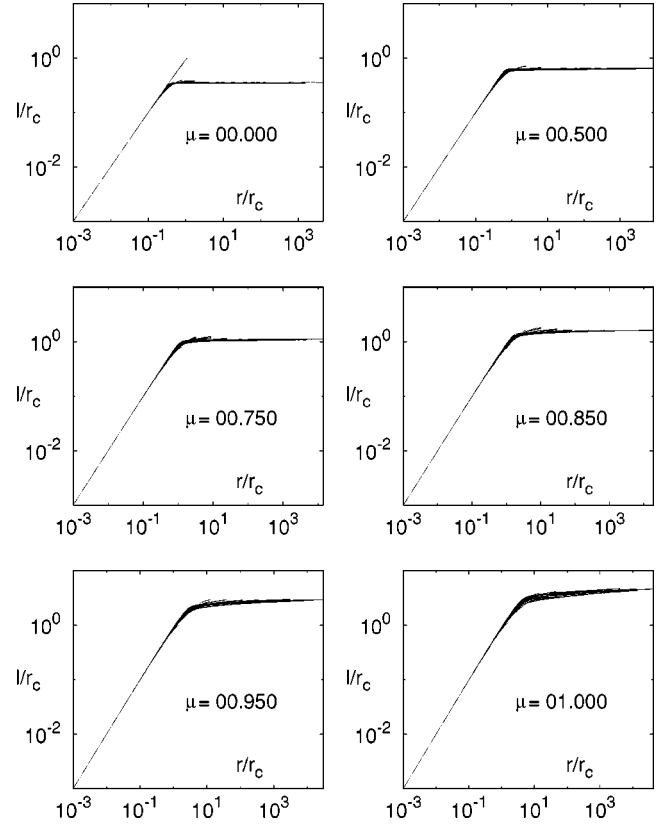

FIG. 10. Shown is ℓ/r_c vs r/r_c, with $r_c = p^{-1} \ln(4(pL)^{(1-\mu)})/\ln(4)$. The density of LR bonds is $p = 0.001$, 0.003, and 0.01. System sizes L are of the form $L_k = 10^{3+k/2}$ with $k = 0,1,\ldots,8$. The proposed expression for r_c has only been justified theoretically for $\mu = 0$ [32,44], and is purely empirical for $0 < \mu < 1$.

(see the beginning of Sec. III) $P_l = \ln[(l+1)/l]/\ln(L)$, from which $G(x) \approx x/\ln(L)$. Thus Eq. (16) can be written approximately as

$$\ell_n^{(\mu=1)}(r) = 1 + \int_1^r \frac{dx}{1 + x/r_c}, \tag{26}$$

where $r_c = p^{-1} \ln(L)$. Thus naive paths are determined, in the $\mu \to 1$ limit, by a logarithmically L-dependent characteristic size r_c and a logarithmic behavior $\ell(r) \sim \ln(r)$ above r_c. Given that actual shortest-paths must be shorter than naive paths, we conclude that $\ell(r)$ is logarithmic for all $\mu < 1$.

IV. CONCLUSIONS

We considered shortest paths on d-dimensional lattices of L^d sites supplemented with pL^d long-range connections whose lengths l are random variables with power-law distribution $P(l) \sim l^{-\mu}$. We call these networks, since it is the probability to have a LR bond of length l, and not its strength, what decays with distance. The limit $\mu \to 0$ is the "small-world" network of Watts and Strogatz [39]. Under a rescaling transformation with scale parameter b in d dimensions, a small local density p of LR bonds transforms as $\tilde{p}$

$=b^{2d-\mu}p$. In the (μ,p) plane, $p=0$ is a repulsive fixed line for $\mu<2d$ and an attractive fixed line for $\mu>2d$. Thus rescaling arguments predict $\mu_c=2d$ to be a critical decay rate above which LR bonds are irrelevant. Particularizing to $d=1$, a directed model that gives an upper bound for shortest paths can be analytically solved (Sec. II B) and has three regions in the μ axis: (a) $\ell(r)\propto r$ for $\mu>2$, (b) $\ell(r)\propto r^{\mu-1}$ for $1<\mu<2$, and (c) $\ell(r)$ logarithmic for $\mu<1$. In accordance with rescaling arguments, we find numerically that in one dimension $\mu=2$ is a critical point separating a "short-range phase" $(\mu>2)$ where shortest-path lengths are linear, $\ell(r)\propto r$, from a "long-range phase" $(\mu<2)$ where shortest-path lengths are sublinear, $\ell(r)\propto r^{\theta_s}$ with $\theta_s<1$. Our finding that $\mu_c=2$ for all p is consistent with previous work of Jespersen and Blumen [35], but is in disagreement with recent claims of Sen and Chakrabarty [36] who suggest the existence of a p-dependent boundary $\mu^*(p)$. We showed that this apparent boundary is a finite-size effect, due to the fast growth of a correlation length ξ as $\mu\to2^-$.

For small p and $1\le\mu\le2$, a characteristic size $\xi=p^{-\nu}$ with $\nu=1/(1-\mu)$ dictates the shortest path properties. For $r<\xi$ one has $\ell(r)\approx r$ while for $r\gg\xi$, $\ell(r)\sim r_s^\theta(\mu)$ is found. This divergence in the correlation length exponent ν as $\mu\to2^-$ is of the same kind as reported for spin models previously [4,8,13].

For $\mu<1$ the characteristic size behaves as p^{-1} but is also L dependent and we find that Eq. (25) provides a good empirical fit of both its p and L dependence.

The asymptotic exponent θ_s is found numerically to attain its short-range value $\theta_s=1$ for $\mu>2$. It is discontinuous at $\mu=2$, where it probably takes a value near $1/2$, and then goes to zero smoothly as $\mu\to1^+$. For $\mu\le1$ we find logarithmic (or mean-field) behavior: $\theta_s=0$ and $\ell(r)\sim\ln(r)$ asymptotically. For $\mu\to0$ $\ell(r)$ saturates at large distances to a value that depends logarithmically on system size [32,44,47].

ACKNOWLEDGMENTS

APPENDIX: SHORTCUT DISTRIBUTION

1. Normalization

The scale-invariant shortcut distribution $p(r)$ Eq. (4) can be approximated by $p(r)\approx1$ for $r<r_c=\rho^{1/\mu}$ and $p(r)\approx\rho/r^\mu$ for $r>r_c$. Thus the normalization condition Eq. (6) can be written as

$$p=S_d\begin{cases}\int_1^{r_c}r^{d-1}dr+\rho\int_{r_c}^L r^{d-1-\mu}dr & \text{for} \quad r_c>1,\\[2mm]\rho\int_1^L r^{d-1-\mu}dr & \text{for} \quad r_c<1,\end{cases}$$
$$\text{(A1)}$$

so that if $V_d=S_d/d$ is the volume of a unit radius sphere,

$$p=V_d\begin{cases}\dfrac{\rho dL^{d-\mu}}{d-\mu}-\dfrac{\mu\rho^{d/\mu}}{d-\mu}-1 & \text{for} \quad \rho>1,\\[3mm]\dfrac{\rho d(L^{d-\mu}-1)}{d-\mu} & \text{for} \quad \rho<1.\end{cases}$$
$$\text{(A2)}$$

When $\mu<d$ and if p remains finite in the $L\to\infty$ limit one has that

$$\rho=p\frac{d-\mu}{S_d}L^{-(d-\mu)}.\qquad\text{(A3)}$$

This goes to zero for large L, which justifies the power-law approximation Eq. (7). For $\mu>d$ on the other hand, and assuming p small,

$$\rho=p\frac{\mu-d}{S_d},\qquad\text{(A4)}$$

so that the power-law approximation holds for any finite p when $\mu<d$ but only for p small when $\mu>d$. The power-law distribution is properly normalized when

$$1=C\int_1^L r^{d-1-\mu}dr\to C=\frac{(\mu-d)L^{\mu-d}}{S_d(L^{\mu-d}-1)},\qquad\text{(A5)}$$

therefore, in the limit of large L,

$$p(r)=\begin{cases}\dfrac{(\mu-d)}{S_d}\dfrac{p}{r^\mu} & \text{for} \quad \mu>d,\\[3mm]\dfrac{(d-\mu)}{S_d L^{d-\mu}}\dfrac{p}{r^\mu} & \text{for} \quad \mu<d,\end{cases}$$
$$\text{(A6)}$$

gives the probability for two sites separated by an Euclidean distance r to be connected by a LR bond.

2. Rescaling

From the rescaling of ρ, Eq. (3), and the relationships (A3) and (A4) between ρ and p it is immediate to conclude that

$$\tilde{p}=b^{y_p}p,\qquad\text{(A7)}$$

with

$$y_p=\begin{cases}d & \text{for} \quad \mu\le d,\\ 2d-\mu & \text{for} \quad \mu>d.\end{cases}$$
$$\text{(A8)}$$

3. Naive paths when $\mu>2$

For $\mu>1$ and $L\gg1$ we have that $P_l=l^{1-\mu}-(l+1)^{1-\mu}$. Using this expression, Eq. (14) gives $G(x)=\Sigma_{l=1}^x(l-1)[l^{1-\mu}-(l+1)^{1-\mu}]=H(x+1,\mu-1)-1-(x+1)^{-\mu}+(x+1)^{-(\mu-1)}$, where $H(x,\alpha)=\Sigma_{l=1}^x 1/l^\alpha$ are called harmonic numbers. $H(x,\alpha)$ can be approximated (within 1% error) for all $\alpha\ge1$ and $x\ge2$ by

$$H(x,\alpha) \approx 1 + 2^{-\alpha} + \frac{3^{-\alpha} + x^{-\alpha}}{2} + \frac{x^{1-\alpha} - 3^{1-\alpha}}{1-\alpha}. \quad \text{(A9)}$$

Within this approximation one obtains $(\bar{l}-1) = H(\infty, \mu - 1) - 1 = 2^{1-\mu} + (3^{1-\mu})/2 + (3^{2-\mu})/(\mu-2)$, which is found to be very accurate for all $\mu \geq 2$. Using this approximate expression, Eq. (19) can be integrated to give

$$\Phi(r) = \frac{(\bar{l}-1)(r-1)}{r} - \frac{Z(r, 3-\mu)}{r(\mu-2)} + \frac{3Z(r, 2-\mu)}{2r}$$

$$- \frac{Z(r, 1-\mu)}{r}, \quad \text{(A10)}$$

where $Z(x, \alpha) = [(x+1)^{\alpha} - 2^{\alpha}]/\alpha$.

---

[1] D.J. Thouless, Phys. Rev. **187**, 732 (1969).

[2] F.J. Dyson, Commun. Math. Phys. **21**, 269 (1971).

[3] M. Fisher, S. Ma, and B. Nickel, Phys. Rev. Lett. **29**, 917 (1972).

[4] J.M. Kosterlitz, Phys. Rev. Lett. **37**, 1577 (1976).

[5] J.L. Monroe, Phys. Lett. A **171**, 427 (1992).

[6] S.A. Cannas, Phys. Rev. B **52**, 3034 (1995).

[7] E. Luijten and H. Blote, Phys. Rev. Lett. **76**, 3662 (1996).

[8] E. Luijten and H. Blote, Phys. Rev. B **56**, 8945 (1997).

[9] J.L. Monroe, J. Phys. A **31**, 9809 (1998).

[10] E. Bayong and H. Diep, Phys. Rev. B **59**, 11 919 (1999).

[11] D.R. Hamann, Phys. Rev. Lett. **23**, 95 (1969).

[12] P. Anderson and G. Yuval, Phys. Rev. Lett. **23**, 89 (1969).

[13] S. Cannas and A. de Magalhaes, J. Phys. A **30**, 3345 (1997).

[14] Z. Glumac and K. Uzelac, J. Phys. A **26**, 5267 (1993).

[15] J.L. Monroe, J. Phys. A **32**, 7083 (1999).

[16] E. Bayong, H. Diep, and V. Dotsenko, Phys. Rev. Lett. **83**, 14 (1999).

[17] Y. Wang and P. Schlottmann, Phys. Rev. B **63**, 134437 (2001).

[18] S. Romano and R. Sokolovskii, Phys. Rev. B **61**, 11 379 (2000).

[19] S. Feng and X. Qiu, Commun. Theor. Phys. **30**, 129 (1998).

[20] S. Romano, Int. J. Mod. Phys. B **10**, 1095 (1996).

[21] S. Romano, Phys. Rev. B **46**, 5420 (1992).

[22] S. Fakioglu, Nuovo Cimento Soc. Ital. Fis., D **10D**, 1161 (1988).

[23] F. Tamarit and C. Anteneodo, Phys. Rev. Lett. **84**, 208 (2000).

[24] H. Rieger and F. Igloi, Phys. Rev. Lett. **83**, 3741 (1999).

[25] R.T. Scalettar, Physica A **170**, 282 (1991).

[26] B. Chakrabarti, A. Maggs, and R. Stinchcombe, J. Phys. A **18**, L373 (1985).

[27] D. Chowdhury and B. Chakrabarti, J. Phys. A **18**, L377 (1985).

[28] S. Xiong, Y. Chen, and S. Evangelou, Phys. Rev. Lett. **77**, 4414 (1996).

[29] Y. Beigelzimer, V. Synkov, L. Trankovskaya, and D. Trankovskii, Powder Metall. Met. Ceram. **36**, 176 (1997).

[30] T. Yang and L. Chua, Int. J. Bifurcation Chaos Appl. Sci. Eng. **9**, 2105 (1999).

[31] L. Lago-Fernandez, R. Huerta, F. Corbacho, and J. Siguenza, Phys. Rev. Lett. **84**, 2758 (2000).

[32] C.F. Moukarzel, Phys. Rev. E **60**, R6263 (1999).

[33] R. Pastor-Satorras and A. Vespignani, Phys. Rev. Lett. **86**, 3200 (2001).

[34] *Fractals and Disordered Systems*, edited by A. Bunde and S. Havlin, 2nd ed. (Springer-Verlag, Heidelberg, 1996).

[35] S. Jespersen and A. Blumen, Phys. Rev. E **62**, 6270 (2000).

[36] P. Sen and B. Chakrabarti, J. Phys. A **34**, 7749 (2001).

[37] J. van Leeuwen, *Handbook of Theoretical Computer Science* (Elsevier, New York, 1990), Chap. 10.

[38] T.H. Cormen, C.E. Leiserson, and R.L. Rivest, *Introduction to Algorithms*, 9th ed. (McGraw-Hill, New York, 1993), Chap. 6.

[39] D. Watts and S. Strogatz, Nature (London) **393**, 440 (1998).

[40] G.B. Lubkin, Phys. Today **51**(9), 17 (1998).

[41] M. Barthelemy and L. Amaral, Phys. Rev. Lett. **82**, 3180 (1999).

[42] M. Newman and D. Watts, Phys. Rev. E **60**, 7332 (1999).

[43] R. Monasson, Eur. Phys. J. B **12**, 555 (1999).

[44] M. De Menezes, C. Moukarzel, and T. Penna, Europhys. Lett. **50**, 574 (2000).

[45] C. Moore and M. Newman, Phys. Rev. E **62**, 7059 (2000).

[46] M. Kuperman and G. Abramson, Phys. Rev. Lett. **86**, 2909 (2001).

[47] M. de Menezes, C. Moukarzel, and T. Penna, Physica A **295**, 132 (2001).